SYNTHESIS, PHYSICOCHEMICAL AND SPECTROPHOTOMETRIC ANALYSIS OF CURCUMIN ANALOGS WITH CYCLOHEXANONE CORE

Zlatko Lozanovski
Higher Medical School, St. Kliment Ohridski University - Bitola, RN Macedonia,
zlatko.lozanovski@uklo.edu.mk
Tatjana Nestorovska
Higher Medical School, St. Kliment Ohridski University - Bitola, RN Macedonia,
tatjana.nestorovska@uklo.edu.mk
Angelka Jankulovska
Higher Medical School, St. Kliment Ohridski University - Bitola, RN Macedonia,
angelka.jankulovska@uklo.edu.mk
Daniela Petkovska
Higher Medical School, St. Kliment Ohridski University - Bitola, RN Macedonia,
daniela.petkovska@uklo.edu.mk
Denis Arsovski
Higher Medical School, St. Kliment Ohridski University - Bitola, RN Macedonia,
denis.arsovski@uklo.edu.mk

Abstract: Due to the presence of specific functional groups in its structure, curcumin has demonstrated a wide range of therapeutic properties for which it has garnered significant interest over the past twenty years. Despite this, curcumin's low chemical stability owing to keto-enol tautomerism and poor water solubility results in low bioavailability, limit its use in therapy. In this study were synthetized seven curcumin analogs with cyclohexanone core: **Ia, Ib, Ic, IF5NO2, Id, Ie and If.** Analogs were prepared by Claisen-Schmidt condensation reaction between corresponding benzaldehyde and arylaldehyde. Several spectroscopic techniques were used to confirm the structure of the obtained analogs. The effective synthesis and the presence of a conjugated dienone system can be inferred from the infrared spectra. The analogs color, which range from light yellow to orange and their UV-Vis spectra, which have λ_{max} values above 300 nm, further substantiate the extended conjugation indicating that there are several double bonds adjacent, and their bonding orbitals can interact and form one huge delocalized system. From the infrared spectra it can be seen that analogs exhibited an absorption band below 1700 cm^{-1}, which is likewise consistent with the literature and suggests the existence of a conjugated carbonyl group. As part of this paper, chromatographic methods (HPLC-DAD-MS) were applied to determine the purity of the synthesized curcumin analogues with cyclohexanone core. These analogues can further be tested and analyzed in terms of their cytotoxicity or therapeutic potency.
Keywords: synthesis; analogs of curcumin; cyclohexanone core; conjugated carbonyl group.

1. INTRODUCTION

In the last 20 years, curcumin has been intensively investigated by a large number of scientists in order to prove its therapeutic effects against malignant diseases, autoimmune diseases, metabolic, neurological, cardiovascular, pulmonary and inflammatory diseases (Aggarwal et al., 2009; Kannappan et al., 2011). It has been found to play an important role in the regulation of cytokines, kinases, enzymes, transcription factors, growth factors, receptors, metastatic and apoptotic molecules in almost all stages of the development of many diseases (Baliga et al., 2012; Prasad et al., 2014; Shehzad et al., 2010). The antioxidant properties of curcumin are attributed to its structure prone to methoxylation versus hydrogenation and free radical scavenging ability (Liu et al., 2018). Although the beneficial biological activities in the curcumin molecule are due to the electrophilic nature of the central β-diketo and methylene group - it has been established that their high reactivity cause chemical instability at pH above 6.5 and rapid degradation (Anand et al., 2007; Tomren et al., 2007).

The presence of relatively acidic hydrogen atoms in the curcumin molecule leads to an intramolecular transfer of proton(s), and thus the appearance of keto and enol tautomers that are in equilibrium, figure 1.

In the keto form of curcumin, the heptadienone bond between the two methoxy phenolic rings contains a highly activated C atom whose C-H bonds are very weak as a result of the delocalization of the lone electron pair from nearby oxygen atoms. However, in certain situations, for example at pH > 8, the enol form prevails in the heptadienone chain, whereby the curcumin molecule acts as an electron donor.

Figure 1. Keto–enol tautomerism in curcumin

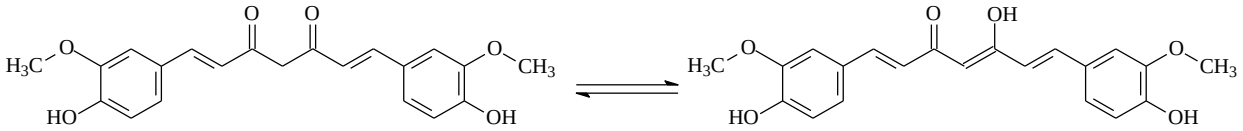

Source: (Jankun et al., 2016)

In order to increase the bioavailability of curcumin, improve the chemical stability, reduce rapid metabolism and improve the systemic delivery of curcumin in the body, modeling of the structure of curcumin is approached. There are several general strategies that are based on the elimination of potential sites for oxidation (phenolic and enol hydroxyl groups) and enrichment with functional groups, i.e. atoms - because with the elimination of enol and phenolic hydroxyl groups, the intermolecular bonds are broken, cause weakening the biological and pharmacological characteristics therefore required that newly synthesized analogs be "enriched" with functional groups or atoms that will be capable of interactions with target receptors (such as cancer cells) (Robinson et al., 2005; Fuchs et al., 2009; Liang et al., 2009). As one of the more frequently applied techniques is modification in the central β-diketo and methylene group (which are the causes of its chemical instability) and obtaining analogs containing an electrophilic α,β-unsaturated carbonyl group (Michael acceptors) responsible for many key biological processes through the process of thiol-alkylation (glutathione, cysteine, peptides with cysteine groups) (Lozanovski et al., 2023).

2. MATERIALS AND METHODS

Reagents

Cyclohexanone, 4-bromobenzaldehyde, 5-nitro-2-furfuraldehyde, 2-methylbenzaldehyde, 2,5-dimethylbenzaldehyde, 2-methoxybenzaldehyde, 4-methylbenzaldehyde, 4-dimethylbenzaldehyde, acetonitrile (HPLC purity) were purchased from Sigma Aldrich. Ammonium chloride, methanol, chloroform and sodium hydroxide were from Fisher Chemical and ethanol was purchased from AD Alkaloid Skopje.

Instrumentation

Melting temperatures was obtained using a Mel-Temp melting point apparatus, and they weren't corrected. Using a KBr pellet, infrared spectra were obtained using a Varian Excalibur 3100 FT-IR spectrometer. Cary 50 spectrophotometer was used to obtain *the absorbance spectra of analogs*. An Agilent 1100 HPLC system with an ESI interface was utilized for the mass spectrum measurements, and software (Agilent, v.4.1) controlled an ion-trap mass analyzer for the MS analysis. The measurements were obtained in APCI mode.

UV-Vis spectra of curcumin analogs with cyclohexanone core

UV-Vis spectra were recorded on a Cary 50 spectrophotometer in a quartz cuvette from 200 to 800 nm wavelength. Analogues were weighed to obtain a conc. of 0,2–0,4 mg/mL and then dissolved in spectrophotometrically pure CH_3CN respectively in separate flasks. An appropriate aliquot was taken from these solutions to obtain a 10^{-5} M concentration in pure CH_3CN or 80/20 (*V/V*) CH_3CN/H_2O. The blank was recorded in CH_3CN or 80/20 CH_3CN/H_2O (*V/V*). UV-Vis spectra of analogs were recorded in 80/20 CH_3CN/H_2O (*V/V*) and kept in the dark during all recordings.

Synthesis method for curcumin analogs with cyclohexanone core

The synthesis was performed by adapting the procedure from Qian and coworkers (Qian et al., 2015). The flask was filled with 10 ml of methanol, 15 mmol of arylaldehyde, and 7.5 mmol of the equivalent cyclohexanone. This mixture was stirred for 5 minutes and 2 ml of aqueous NaOH solution was added dropwise over a period of 5 minutes. The mixture thus prepared was stirred for 60 minutes in order to obtain a colored precipitate. The mixture was cooled for 15 minutes in an ice bath and filtered. A precipitate of each combination of arylaldehyde and cyclohexanone was thus obtained and washed simultaneously with saturated aqueous NH_4Cl (15 ml), distilled water (30 ml) and cold CH_3OH (10 ml). We recrystallized the products obtained in this way with the appropriate solvent, which is specified for each analogue in this section.

(2E,6E)-2,6-bis(4-methylbenzylidene)cyclohexanone (Ia): recryst., from $C_4H_8O_2$, yellow needle crystals, yield (58%), T_m 168-170 °C (lit. 171-172 °C (Amoozadeh et al., 2011)); **FT-IR-ATR** (sapphire): 1661 cm^{-1} (C = O); **UV-Vis** : λ_{max} (80/20 $CH_3CN:H_2O$) = 340 nm (ε = 62522 $L \cdot mol^{-1} \cdot cm^{-1}$); **HPLC-DAD-MS**, t_R = 7,9 min; **MS-APCI** (*m*/*z*) = 303 (MH^+).

(2E,6E)-2,6-bis((4-dimethylaminobenzylidene)cyclohexanone (Ib): recryst., from C_2H_5OH, orange crystals, yield (47%),T_m 248-250 °C (lit. 183-184 °C (Kar et al., 2019)**)**; **FT-IR** (KBr): 1645 cm^{-1} (C=O); **UV-Vis**: λ_{max} (80/20 $CH_3CN:H_2O$) = 445 nm (ε = 30847 $L \cdot mol^{-1} \cdot cm^{-1}$); **HPLC-DAD-MS**, t_R = 6,1 min; **MS-APCI** (*m/z*) = 361 (MH^+).
(2E,6E)-2,6-bis(4-bromobenzylidene)cyclohexanone (Ic): recrys., from C_2H_5OH, yellow needle crystals, yield (47%), T_m 165-168 °C (лит. 149-151 °C (Grynkiewicz et al., 2012; Gupta et al. 2011; Priyadarsini et al., 2013); **FT-IR** (KBr): 1672 cm^{-1} (C=O); FT-IR (CCl_4): 1672 cm^{-1} (C=O), FT-IR-ATR (sapphire): 1666 cm^{-1} (C=O); **UV-Vis**: λ_{max} (80/20 $CH_3CN:H_2O$) = 334 nm (453 mAU), 238 nm (209 mAU); **HPLC-DAD-MS**, t_R = 9,2 min; **MS- APCI** (*m/z*) = 433 (MH^+).
(2E,6E)-2,6-bis(5-nitro-2-furfurylidene)cyclohexanone (IF5NO2): recryst., from 96% C_2H_5OH, brown crystals, yield (67%), 214-216 ºC; **FT-IR** (KBr): 1664 cm^{-1} (C=O); **UV-Vis**: λ_{max} (80/20 $CH_3CN:H_2O$) = 396 nm (ε = 41673 $L \cdot mol^{-1} \cdot cm^{-1}$); **HPLC-DAD-MS**, t_R = 2,5 min; **MS-APCI** (*m/z*) = 345 (MH^+).
(2E,6E)-2,6-bis(2-methylbenzylidene)cyclohexanone (Id): recryst., from C_2H_5OH, yellow crystals, yield (58%), T_m 138-140 °C; **UV-Vis**: λ_{max} (80/20 $CH_3CN:H_2O$) = 320 nm (675 mAU), 232 nm (312 mAU); **HPLC-DAD-MS**, t_R = 6,9 min; **MS-APCI** (*m/z*) = 303 (MH^+).
(2E,6E)-2,6-bis(2,5-dimethylbenzylidene)cyclohexanone (Ie): recryst., from C_2H_5OH, yellow crystals, yield (76%), T_m 135-137 °C **FT-IR** (KBr): 1666 cm^{-1} (C = O); **UV-Vis**: λ_{max} (80/20 $CH_3CN:H_2O$) = 308 nm (930 mAU), 238 nm (514 mAU)
(2E,6E)-2,6-bis(3,4-dimethoxybenzylidene)cyclohexanone (If): recryst., C_2H_5OH, yellow crystals, yield (58%), **UV-Vis**: λ_{max} (80/20 $CH_3CN:H_2O$) = 376 nm (1191 muA) 254 nm (514 muA) **FT-IR-ATR** (сафир): 1654 cm^{-1} (C = O); **HPLC-DAD-MS**, t_R = 2,9 min; **MS-ESI** (*m/z*) = 395 (MH^+).

3. RESULTS AND DISCUSSION

Seven analogues of curcumin with a cyclohexanone core (**Ia, Ib, Ic, IF5NO₂, Id, Ie and If)** were synthesized through the Cleisen-Schmidt reaction between the corresponding aromatic aldehyde and cyclohexanone in an alkaline medium, resulting in the elimination of the β-diketo group from curcumin and its transformation into a mono-keto group that would have higher stability in the newly synthesized analogs relative to curcumin, figure 2.

Figure 2. Synthesis of curcumin analogs with a cyclohexanone core: Ia (2E,6E)-2,6-bis(4-methylbenzylidene)cyclohexanone, Ib (2E,6E)-2,6-bis((4-dimethylamino)benzylidene)cyclohexanone, Ic (2E,6E)-2,6-Bis(4-bromobenzylidene)cyclohexanone, IF5NO₂ (2E,6E)-2,6-bis(5-nitro-2-furfulidene)cyclohexanone, Id (2E,6E)-2,6-bis(2-methylbenzylidene)cyclohexanone, Ie (2E,6E)-2,6-bis(2,5-dimethylbenzylidene)cyclohexanone, If (2E,6E)-2,6-bis(3, 4-dimethoxybenzylidene)cyclohexanone.

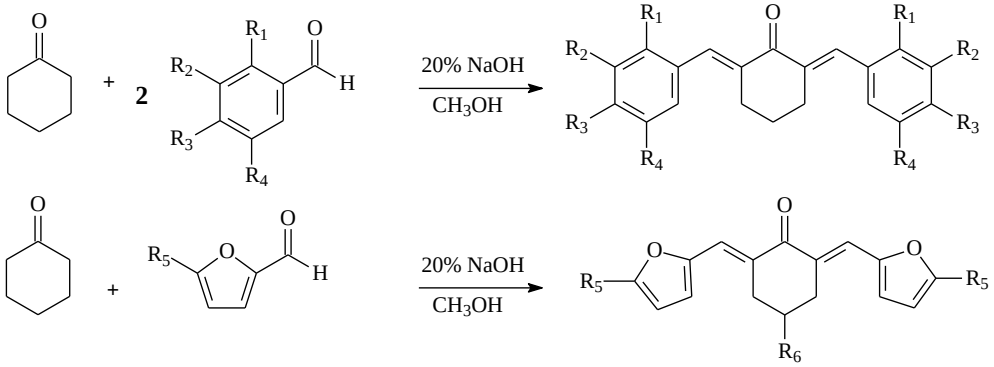

Ia : $R_1 = H$; $R_2 = H$; $R_3 = CH_3$; $R_4 = H$
Ib : $R_1 = H$; $R_2 = H$; $R_3 = N(CH_3)2$; $R_4 = H$
Ic : $R_1 = H$; $R_2 = H$; $R_3 = Br$; $R_4 = H$
IF5NO₂ : $R_5 = NO_2$; $R_6 = H$
Id : $R_1 = H$; $R_2 = CH_3$; $R_3 = H$; $R_4 = H$
Ie : $R_1 = CH_3$; $R_2 = H$; $R_3 = H$; $R_4 = CH_3$
If : $R_1 = H$; $R_2 = OCH_3$; $R_3 = OCH_3$; $R_4 = H$

Source: Author

In Table 1, are summarized and shown several important physicochemical and spectroscopic data for the synthesized analogs of curcumin with a cyclohexanone core.

Table 1. Several important physicochemical and spectroscopic data for the synthesized analogs of curcumin (Ia, Ib, Ic, IF5NO$_2$, Id, Ie and If) with a cyclohexanone core.

Analogs	T_m (°C)	FT-IR (KBr): cm^{-1}	FT-IR-ATR (сафир) cm^{-1}	UV-VIS $\lambda_{max\,1}$ (80/20 CH_3CN: H_2O)	UV-VIS $\lambda_{max\,2}$ (80/20 CH_3CN: H_2O)	HPLC-DAD-MS, t_R (min)	APCI-MS *(m/z)*
Ia	168-170 °C	1661 (C = O)	/	340 nm	236 nm	7,9 min	303 (MH^+)
Ib	248-250 °C	1645 (C = O)	/	445 nm	271 nm	6,1 min	361 (MH^+)
Ic	165-168 °C	1672 (C = O)	1666 (C = O)	334 nm	238 nm	9,2 min	433 (MH^+)
1F5NO$_2$	214 -216 °C	1664 (C = O)		396 nm	256 nm	2,5 min	345 (MH^+)
Id	138-140 °C	1661 (C = O)	/	320 nm	232 nm	6,9 min	303 (MH^+)
Ie	135-137 °C	/	1670	325 nm	228 nm	8,2 min	331 (MH^+)
If	143-145 °C	/	/	376 nm	253 nm	2,9 min	395 (MH^+)

Source: Author

The resulting analogues were recrystallized from the appropriate solvents, and their melting points were determined and compared with the literature. The conjugation is additionally supported by the color of the derivatives (light yellow to orange), table 1.

In all analogs, an absorption band below 1700 cm^{-1} is observed, indicating the presence of a conjugated carbonyl group. At **Ia**, a sharp and intense peak with medium intensity at 1661 cm^{-1} originating from the C=O group is evident. The bands at 2940 and 2860 cm^{-1} in **Ia** originate from alkane -C-H bonds in which the carbon atom is sp^3 hybridized. This peak is most likely due to the CH_3 groups of the benzene ring, figure 3.

Figure 3. FT-IR-ATR spectrum of 2,6-bis(4-methyldibenzylidene)cyclohexanone Ia recrystallized from ethyl acetate.

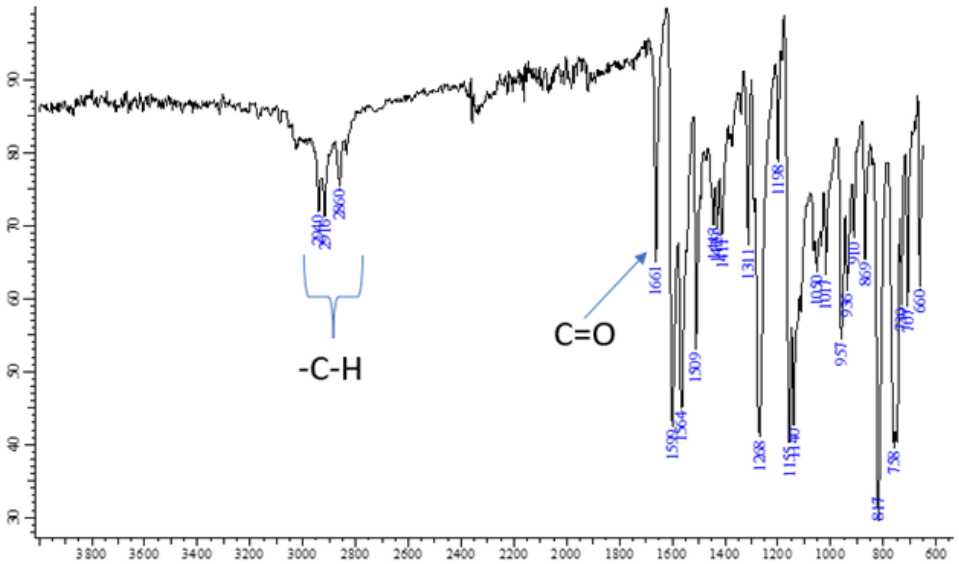

Source: Author

Extensive conjugation is further supported by UV-Vis spectra data for all analogs ($\lambda_{max}(CH_3CN/H_2O)$ = 320- 445 nm), figure 4.

Figure 4. Representative UV-VIS spectra of Ia, Ib, IF5NO2 and Ie dissolved in 80/20(V/V) CH3CN/H2O (quartz cuvette), respectively.

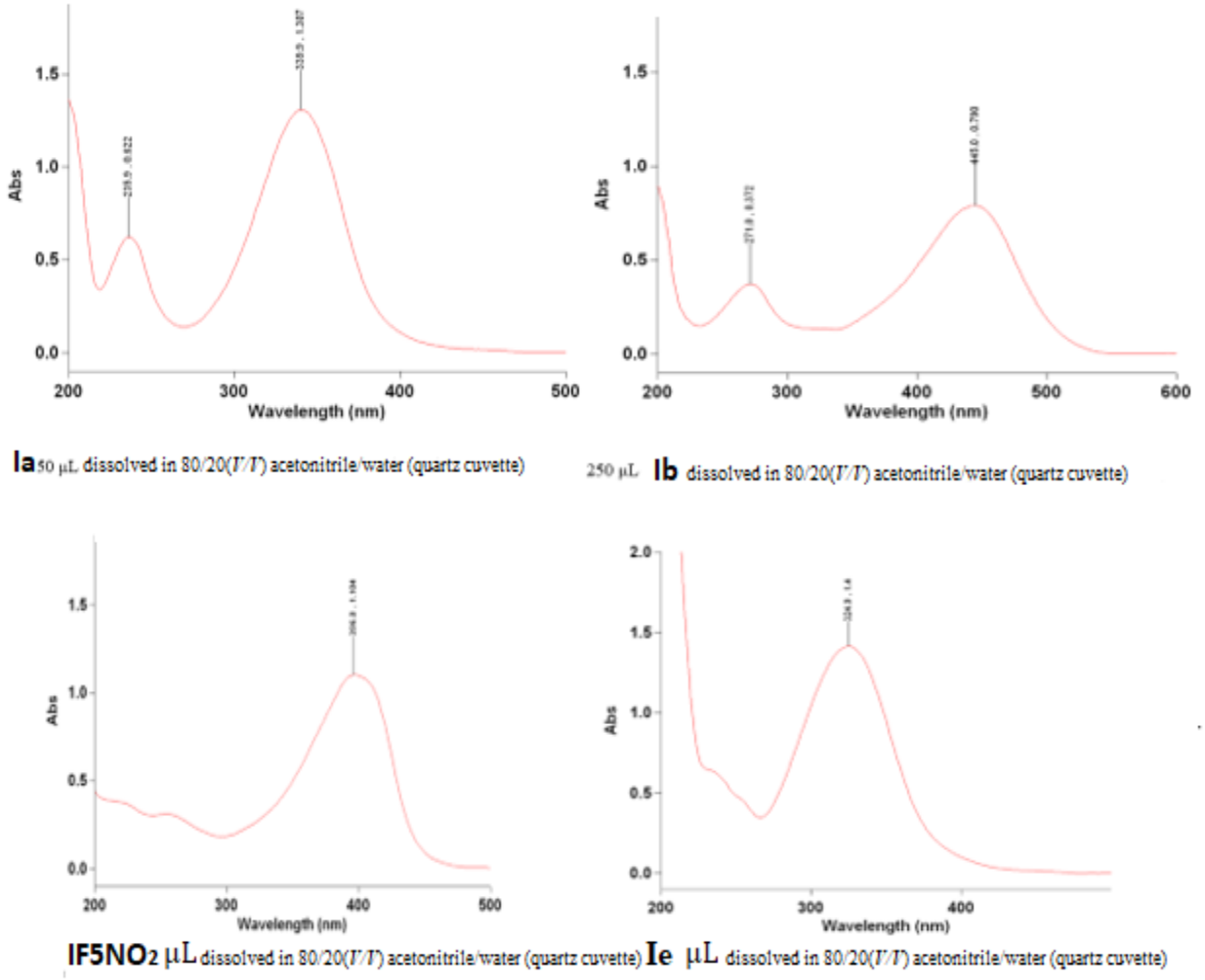

Source: Author

From the UV-VIS spectra of all compounds in CH_3CN/H_2O sumurized in Table 1 and shown in Figure 4, it can be noted that they show two maxima. First maximum at a longer wavelength (320-445 nm) corresponding to the n→π* transition and the second maximum at lower wavelengths (228-271 nm) originating from a π→π* transition. This is consistent with previous UV-Vis studies of monocarbonyl curcumin analogs (Fomina et al., 2022) and further substantiate the extended conjugation indicating that there are several double bonds adjacent, and their bonding orbitals can interact and form one huge delocalized system that can further initiate the attraction or repulsion of the electron pair from the targeted nucleophile or electrophile which may be the subject of other research.

As a final confirmation of the exact structure of the analogs is the mass spectrum, obtained by APCI-MS, table 1, where a protonated molecular ion at 303 amu (MH^+) is observed in **Ia** Figure 5.

Figure 5. HPLC-DAD-MS analysis of Ia, t_R = 7,9 min; λ_{max} (80/20 (V/V) CH_3CN/H_2O) = 340 nm (27,6 mAU), 236 nm (12,7 mAU); APCI-MS (m/z) = 275 (MH^+); APCI-MS^2

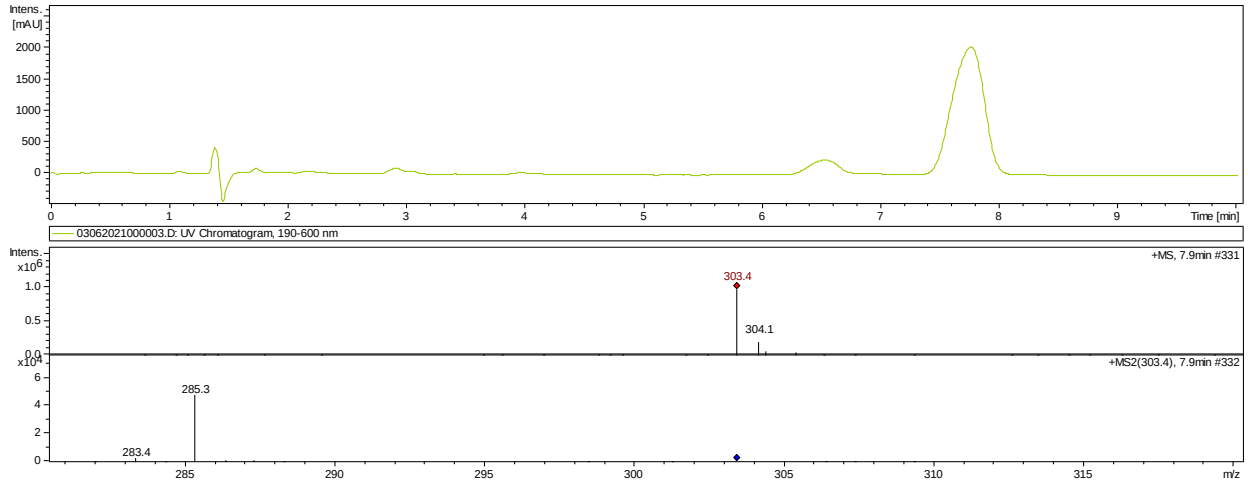

Source: Author

4. CONCLUSIONS

We synthesized seven analogues, purified and characterized them. The resulting analogues were recrystallized from the appropriate solvents, and their melting points were determined and compared with the literature. The structure of the obtained analogues was confirmed by several spectroscopic methods. From the infrared spectra it can be concluded that the compounds have been successfully synthesized and that they contain a conjugated dienone system. The extensive conjugation is additionally supported by the color of the derivatives (light yellow to orange) as well as by their UV-Vis spectra (λmax above 300 nm). In all analogs, an absorption band below 1700 cm^{-1} is observed, indicating the presence of a conjugated carbonyl group, which is also in agreement with the literature. It was necessary to investigate the solubility of the newly obtained analogues in solvents suitable for UV-Vis analysis such as (C_2H_5OH, CH_3CN, CH_2Cl_2, $(CH_3)_2SO$, CH_3OH, $C_2H_6O_2$, etc.), taking into account that the choice of solvent would be compatible for subsequent HPLC analyses. The next key criterion was that the solvent be miscible in water in order to be able to add a buffer or other water-soluble solvent. We found exactly such a combination of two solvents to be suitable for our analyzes according to the obtained UV-VIS spectra, i.e. a combination of 80/20 (*V/V*) CH_3CN/H_2O. The advantage of this research is enabling next steps in structural investigations and semi-empirical computational methods that would give a more complete picture in the assessment of reactivity, factors and mechanisms of action of these biologically active analogs.

REFERENCES

Aggarwal, B. B., & Harikumar, K. B. (2009). Potential therapeutic effects of curcumin, the anti-inflammatory agent, against neurodegenerative, cardiovascular, pulmonary, metabolic, autoimmune and neoplastic diseases. *The international journal of biochemistry & cell biology*, *41*(1), 40–59. https://doi.org/10.1016/j.biocel.2008.06.010.

Amoozadeh, A., Rahmani, S., Dutkiewicz, G. (2011). Novel Synthesis and Crystal Structures of Two α, α′-bis-Substituted Benzylidene Cyclohexanones: 2,6-Bis-2-nitro(benzylidene)cyclohexanone and 2,6-Bis-4-methyl(benzylidene)cyclohexanone. *Journal of Chemical Crystallography*, 41,(2), 1305–1309. https://doi.org/10.1007/s10870-011-0094-7.

Anand, P., Kunnumakkara, A. B., Newman, R. A., & Aggarwal, B. B. (2007). Bioavailability of curcumin: problems and promises. *Molecular pharmaceutics*, *4*(6), 807–818. https://doi.org/10.1021/mp700113r

Baliga, M. S., Joseph, N., Venkataranganna, M. V., Saxena, A., Ponemone, V., & Fayad, R. (2012). Curcumin, an active component of turmeric in the prevention and treatment of ulcerative colitis: preclinical and clinical observations. *Food & function*, *3*(11), 1109–1117. https://doi.org/10.1039/c2fo30097d.

Fomina, M. V., Vatsadze, S. Z., Freidzon, A. Y., Kuz'mina, L. G., Moiseeva, A. A., Starostin, R. O., Nuriev, V. N., & Gromov, S. P. (2022). Structure-Property Relationships of Dibenzylidenecyclohexanones. *ACS omega*, *7*(12), 10087–10099. https://doi.org/10.1021/acsomega.1c06129.

Fuchs, J. R., Pandit, B., Bhasin, D., Etter, J. P., Regan, N., Abdelhamid, D., Li, C., Lin, J., & Li, P. K. (2009). Structure-activity relationship studies of curcumin analogues. *Bioorganic & medicinal chemistry letters*, *19*(7), 2065–2069. https://doi.org/10.1016/j.bmcl.2009.01.104.

Gupta, S. C., Prasad, S., Kim, J. H., Patchva, S., Webb, L. J., Priyadarsini, I. K., & Aggarwal, B. B. (2011). Multitargeting by curcumin as revealed by molecular interaction studies. *Natural product reports*, *28*(12), 1937–1955. https://doi.org/10.1039/c1np00051a.

Jankun, J., Wyganowska-Świątkowska, M., Dettlaff, K., Jelińska, A., Surdacka, A., Wątróbska-Świetlikowska, D., & Skrzypczak-Jankun, E. (2016). Determining whether curcumin degradation/condensation is actually bioactivation (Review). International Journal of Molecular Medicine, 37, 1151-1158. https://doi.org/10.3892/ijmm.2016.2524.

Kannappan, R., Gupta, S. C., Kim, J. H., Reuter, S., & Aggarwal, B. B. (2011). Neuroprotection by spice-derived nutraceuticals: you are what you eat!. *Molecular neurobiology*, *44*(2), 142–159. https://doi.org/10.1007/s12035-011-8168-2.

Kar, S.; Ramamoorthy, G.; Sinha, S.; Ramanan, M.; Pola, J.K.; Golakoti, N.R.; Nanubolu, J.B.; Sahoo, S.K.; Dandamudi, R.B.; Doble, M. (2019). Synthesis of Diarylidenecyclohexanone Derivatives as Potential Anti-Inflammatory Leads against COX-2/MPGES1 and 5-LOX. New Journal of Chemistry, 43, 9012–9020. https://doi.org/10.1039/C9NJ00726A.

Liang, G., Shao, L., Wang, Y., Zhao, C., Chu, Y., Xiao, J., Zhao, Y., Li, X., & Yang, S. (2009). Exploration and synthesis of curcumin analogues with improved structural stability both in vitro and in vivo as cytotoxic agents. *Bioorganic & medicinal chemistry*, *17*(6), 2623–2631. https://doi.org/10.1016/j.bmc.2008.10.044.

Liu, Guo-Yun, Cong-Cong Jia, Pu-Ren Han, and Jie Yang. (2018). 3,5-Bis(2-Fluorobenzylidene)-4-Piperidone Induce Reactive Oxygen Species-Mediated Apoptosis in A549 Cells. *Medicinal Chemistry Research: An International Journal for Rapid Communications on Design and Mechanisms of Action of Biologically Active Agents* 27(1): 128–36. https://doi.org/10.1007/s00044-017-2056-x.

Lozanovski, Z., Petreska Stanoeva, J., & Bogdanov, J. (2023). Development of a spectrophotometric method for assessment of the relative reactivity of monocarbonyl analogs of curcumin with 2-(dimethylamino)ethanethiol. *Macedonian Journal of Chemistry and Chemical Engineering*, *42*(1), 13–24. https://doi.org/10.20450/mjcce.2023.2638.

Prasad, S., Gupta, S. C., Tyagi, A. K., & Aggarwal, B. B. (2014). Curcumin, a component of golden spice: from bedside to bench and back. *Biotechnology advances*, *32*(6), 1053–1064. https://doi.org/10.1016/j.biotechadv.2014.04.004.

Priyadarsini K. I. (2013). Chemical and structural features influencing the biological activity of curcumin. *Current pharmaceutical design*, *19*(11), 2093–2100. https://doi.org/10.2174/138161213805289228.

Qian, Y., Zhong, P., Liang, D., Xu, Z., Skibba, M., Zeng, C., Li, X., Wei, T., Wu, L., & Liang, G. (2015). A newly designed curcumin analog Y20 mitigates cardiac injury via anti-inflammatory and anti-oxidant actions in obese rats. *PloS one*, *10*(3), e0120215. https://doi.org/10.1371/journal.pone.0120215.

Robinson, Thomas Philip, Richard B. Hubbard 4th, Tedman J. Ehlers, Jack L. Arbiser, David J. Goldsmith, and J. Phillip Bowen. (2005). Synthesis and Biological Evaluation of Aromatic Enones Related to Curcumin. *Bioorganic & Medicinal Chemistry* 13(12): 4007–13. https://doi.org/10.1016/j.bmc.2005.03.054.

Shehzad, A., and Y. S. Lee. (2010). Curcumin: Multiple Molecular Targets Mediate Multiple Pharmacological Actions: A Review. *Drugs of the Future* 35(2): 113. DOI:10.1358/dof.2010.035.02.1426640.

Tomren, M. A., Másson, M., Loftsson, T., & Tønnesen, H. H. (2007). Studies on curcumin and curcuminoids XXXI. Symmetric and asymmetric curcuminoids: stability, activity and complexation with cyclodextrin. *International journal of pharmaceutics*, *338*(1-2), 27–34. https://doi.org/10.1016/j.ijpharm.2007.01.013.

https://www.researchgate.net/publication/24041235_Exploration_and_synthesis_of_curcumin_analogues_with_improved_structural_stability_both, 2024

https://www.ncbi.nlm.nih.gov/pmc/articles/PMC6270789/, 2024

https://www.researchgate.net/figure/Structures-of-curcumin-and-some-curcumin-analogues_fig1_303559479, 2024